AWR: Anticipate, Withstand, and Recover Resilience Metric for Operational and Planning Decision Support in Electric Distribution System

Gowtham Kandaperumal, *Member, IEEE*, Shikhar Pandey, *Member, IEEE*, and Anurag Srivastava, *Senior Member, IEEE*

***Abstract*—With the increasing number of catastrophic weather events and resulting disruption in the energy supply to essential loads, the distribution grid operators' focus has shifted from reliability to resiliency against high impact, low-frequency events. Given the enhanced automation to enable the smarter grid, there are several assets/resources at the disposal of electric utilities to enhances resiliency. However, with a lack of comprehensive resilience tools for informed operational decisions and planning, utilities face a challenge in investing and prioritizing operational control actions for resiliency. The distribution system resilience is also highly dependent on system attributes, including network, control, generating resources, location of loads and resources, as well as the progression of an extreme event. In this work, we present a novel multi-stage resilience measure called the Anticipate-Withstand-Recover (AWR) metrics. The AWR metrics are based on integrating relevant 'system characteristics based factors', before, during, and after the extreme event. The developed methodology utilizes a pragmatic and flexible approach by adopting concepts from the national emergency preparedness paradigm, proactive and reactive controls of grid assets, graph theory with system and component constraints, and multi-criteria decision-making process. The proposed metrics are applied to provide decision support for a) the operational resilience and b) planning investments, and validated for a real system in Alaska during the entirety of the event progression.**

***Index Terms*—Distribution system, graph theory, resilience metrics, resilience planning.**

I. Introduction

RESILIENCE of a power distribution systems (PDS) is determined by various factors, including the size of the PDS, resource mix, network topology, geographical location and associated weather conditions, load types, geopolitical issues, and interdependency to other critical infrastructure. High impact low frequency (HILF) weather and cyber events causing large-scale outages in the PDS are on the rise. Utilities spend a large sum of money on post-event restoration and repairs. Puerto Rico, which saw huge devastation to the power grid after Hurricane Maria, spent \$3.2 billion to construct new poles and feeders and \$4.7 million to repair power plants, both not amounting significant improvement in resilience [1], [2]. The 2021 Texas outage [3] showed how a single low-frequency, high-impact event could shake an entire community to its core pointing to serious deficiencies in reliability-driven planning. However, the lack of a framework to ensure that the next investment contributes towards a higher resiliency in the wake of an event is unavailable. A right mix of pre-event investment and strategical grid-hardening and automation can ensure a reduction in outages caused by such catastrophic events. It can also ensure that post-event restoration time reduces.

In contrast to the concept of reliability, the PDS design in extreme events, which is radial and has low redundancy, impels the application of resilience to loads or portions of the PDS deemed critical. Therefore, we begin with a PDS definition of resilience as the "ability" of the system to anticipate the impact, resist discontinuity of service, or restore service with rapidity, to critical loads in the system" to drive the direction of our work [10], [13]. Critical loads are defined as the loads that are imperative to the welfare and well-being of the citizens and operation of essential services in the region served by the PDS [14]. Traditionally, resilience is achieved by "design", where the infrastructure is made more robust and redundant to withstand the impact of extreme events. These HILF events can be in the physical or the cyber realm with different methodologies and approaches to enhancing a system's resilience in that realm. An important first step in the process of enabling resilience is to define resilience goals and the metrics to measure [15]. Several metrics have been used in the past with approaches varying based on the definition of resilience [16], [17]. In [7], resilience metrics are based on system attributes pertaining to resilience - resourcefulness, rapidity, robustness, and adaptability. Similar metric evaluation approaches are used in [18]. Reference [19] evaluate resilience as a function of the area under the conceptual resilience curves. In [10], a composite scaled resilience metric

Manuscript received March 27, 2021; revised August 20, 2021; accepted September 23, 2021. Date of publication October 13, 2021; date of current version December 23, 2021. This work was supported in part by the U.S. DOE RADIANCE Project and in part by UI-ASSIST DE-IA0000025 Project. Paper no. TSG-00469-2021. *(Corresponding author: Anurag Srivastava.)*

Gowtham Kandaperumal was with the School of Electrical Engineering and Computer Science, Washington State University, Pullman WA 99163 USA. He is now with Regional Engineering, Commonwealth Edison, Chicago, IL 60668 USA (e-mail: gowtham.kandaperumal@comed.com).

Shikhar Pandey was with the School of Electrical Engineering and Computer Science, Washington State University, Pullman WA 99163 USA. He is now with Smart Grid and Innovation, Commonwealth Edison, Chicago, IL 60668 USA.

Anurag Srivastava was with the School of Electrical Engineering and Computer Science, Washington State University, Pullman, WA 99163 USA. He is now with the Computer Science and Electrical Engineering Department, West Virginia University, Morgantown, WV 26506 USA (e-mail: anurag.srivastava@mail.wvu.edu).

Color versions of one or more figures in this article are available at https://doi.org/10.1109/TSG.2021.3119508.

Digital Object Identifier 10.1109/TSG.2021.3119508

TABLE I
SUMMARY OF KEY RELATED WORK FOR RESILIENCE METRICS AND THE PROPOSED METRICS

Ref.	Year	Metrics Introduced	Approach	Domain	Before	During	After
[4]	2017	System Flexibility, Outage Recovery Cost , Outage recovery Capacity	Evaluation of system restoration using metrics	Restoration	×	×	✓
[5]	2018	Resilience - Loads recovered and survived to total loads	Objective based metrics evaluation	Restoration	×	×	✓
[6]	2019	Recovery speed, efficiency and cost	Evaluation of restoration strategies	Restoration	×	×	✓
[7]	2017	FLEP (Φ, Λ, E, Π) Metrics	Operational and Infrastructure metrics for disturbance, post-disturbance, and restorative stage	Planning Infrastructure Proactive	×	✓	✓
[8]	2010	Maximum reduction in system performance over maximum operator loss	Post-contingency loss	Restoration	×	×	✓
[9]	2015	Curve based metrics utilizing failure probability, failure profile and recovery profile	Post event evaluation of resilience and resilience enhancement decision making	Restoration Cost	×	×	✓
[10]	2019	Code based Metrics	Time duration of events affecting system considered	Availability	×	✓	×
[11]	2016	Choquet Integral based metrics	MCDM based metrics	Restoration	×	×	✓
[12]	2016	AHP based metrics	MCDM based metrics	Restoration	×	×	✓
[*]	[*]	AHP, WSM based multiple metrics	MCDM based metrics for all event phases	Planning Operational	✓	✓	✓

* This paper.

is presented that captures the impact and time duration of an outage which predominantly looks at a fraction of unaffected loads to the duration of outages in seconds. In [20], reliability indices (loss of load frequency, loss of load expectation, energy not served) computed for systems after a HILF event is used as event-specific resilience metrics. Table I shows the comparative summary of the various PDS resilience metrics proposed and introduces developed AWR metrics and its novelty.

The challenge in using resilience metrics existing in literature is that the system's resilience factors vary with the progression of the event. For each stage, the resilience of the system correlates to different characteristics of the system and by not considering these characteristics based on the progression of events leads to overlooked resilience evaluation that may fail to ensure system performance. A prime example of this oversight in evaluating resilience for all stages of event progression was seen during the 2021 Texas blackouts. High emphasis on the ensuring robustness and resourcefulness in the Texas grid lead to the unrealistic performance expectations that failed due to the lack of situational awareness to the threats facing the Texas grid. Before the event (blue sky), the system benefits from situational awareness, increased preparedness, and predictive functions that alert the operator to an impending extreme event. During the event (black sky), the nature of resilience relies on the system's robustness to withstand and successfully absorb impact of the event. The terms "blue sky" and "black sky" days refer to normal operating conditions for the utilities and extraordinary and hazardous catastrophes that affect the system in question as defined in [21], [22]. After the event (grey sky), where the extreme event has subsided, the system's resilience is derived from successful restoration and system state reverting to blue sky operation. For each stage, we present a metric that captures the central property of resilience most applicable to that phase of event progression called the Anticipate-Withstand-Recover or the AWR metric. We also propose, how operational decision for control actions and planning decisions to direct investments can be taken for selecting appropriate resilience improving technologies using the developed metrics. As a result, we aim at providing the contextual framework for resiliency planning and operational support to help utilities design a metrics driven investment strategy and control actions, that maximizes grid resiliency. The resilience metric framework presented in this work is developed: (a) to improve situational awareness and anticipation of vulnerabilities and capabilities before the event, (b) to increase robustness and resourcefulness during the event, and (c) the rapidity and recoverability of the system after the event. The overall complexity of the system plays an important role in the selection of the appropriate resilience factors presented in this work and are intended to be modified appropriately for different systems. In this work, the real world isolated distribution system has been studied as a case study for resilience improvements for multiple scenarios including: a) Battery Energy Storage System (BESS) to alleviate generation stress, and b) Automated Switching for improved system reconfiguration.

Our original contributions in this work allow PDS operators and engineers to use a multi-stage resilience metric to plan, monitor, and operate the PDS for enhanced resilience. The proposed AWR metric is intuitive, flexible and comprehensible. The key contributions of this work are.

1) Formulated a novel resilience framework that can be used to monitor system resiliency before, during, and after an extreme event through Anticipate, Withstand and Recover (AWR) metrics considering event progression and changing system characteristics.
2) Developed relevant factors impacting resiliency based on system characteristics and attributes in each stage of event progression using theoretical concepts from the national emergency preparedness paradigm, graph theory, power engineering and multi-criteria decision making (MCDM).

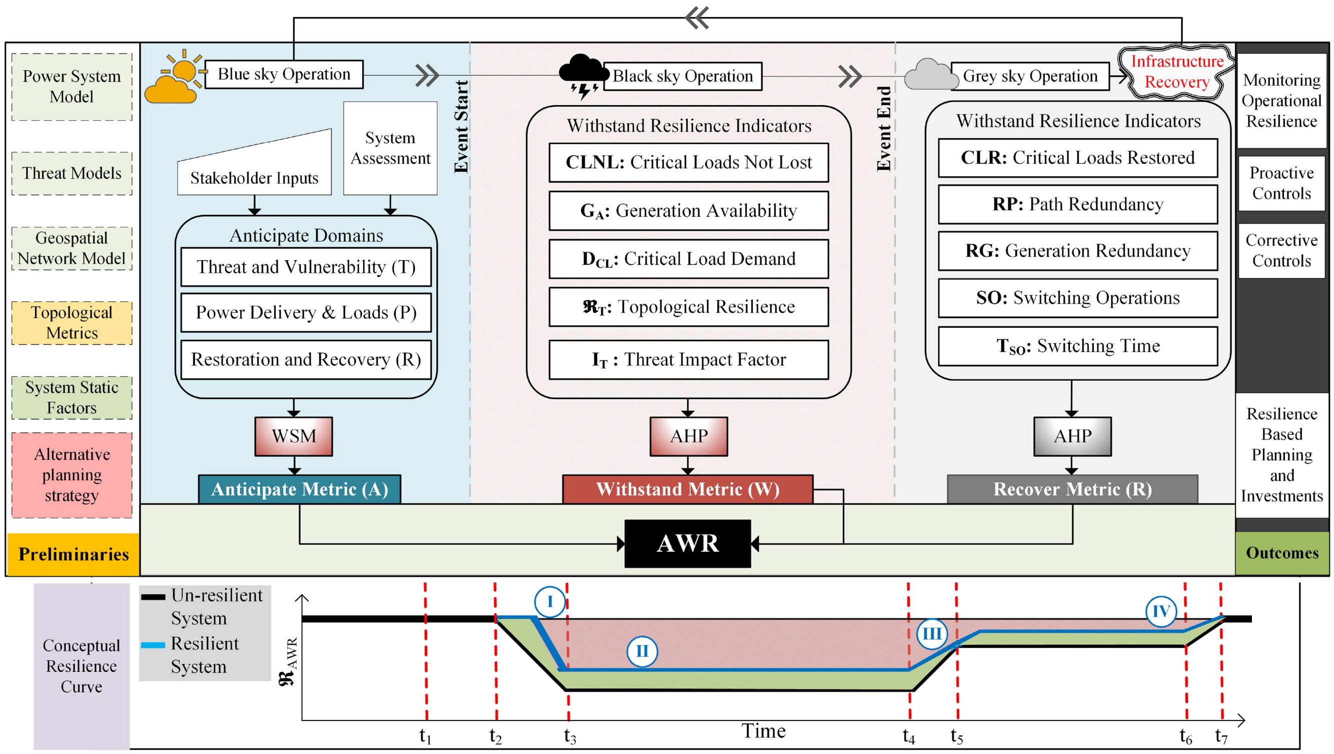

Fig. 1. Overview of Proposed Work to Compute AWR metrics. The conceptual resilience curve shows the outcomes of the proposed work as follows: I. Delayed impact on the system, II. Reduced impact on the system, III. Enhanced performance of recovery, IV. Better post-event performance. The time stamps are as follows: t_1 - start of proactive actions due to better anticipate metric, t_2 - actual event start t_3 - event strikes and system degraded state, t_4 - start system restoration, t_5 - system post-recovery degraded state and begin assessment of infrastructure recovery, t_6 - start infrastructure recovery, and t_7 - pre-event resilience performance.

3) Developed a multi-domain resiliency preparedness checklist to study static resilience factors
4) Developed a decision theory based computation of resiliency scores given multiple factors using Analytical Hierarchical Process and Weighted Sum Model (WSM).
5) Developed a two-stage process to assist planning efforts to target investments in relevant technology for enhanced resilience.

II. AWR Resilience Metrics Formulation

Multi-temporal resilience framework is developed for a real world distribution system, referred to hereinafter as RWS, with well defined threats and utilize the resilience metrics formulated to evaluate the different resilience enabling technologies and available control options. The engineering design of the system limits the types of actions that the Distribution Network Operator (DNO) can perform during the extreme event and therefore, informs the selection of resilience factors required to assess the system. The key assumptions in this work are:

1) *Threat Modeling:* There are deterministic and probabilistic models of damage to the power grid in response to an extreme event. Probabilistic models of damage to power grid like fragility curve based models presented in [23], [24] help to model the impact of wind storms on power poles. The total probability of failure can then be evaluated by a sequential Monte-Carlo analysis. Similarly, statistical tools can be used to derive node and area probability of failure using historical data [25]. Predictive data-driven techniques using machine learning are also options for damage modeling [26]. A catalog of hazards and associated modeling paradigm are presented in [27]. In this work, we consider that the threats are well-defined and modeled explicitly in terms of nodes and lines damaged. The deterministic threat models used in this work are elaborated in Section II-A.
2) *Elicitation:* We present some assessment for resilience goals in the form of expert elicitation with stakeholders to find relevant factors in each domain of interest. The reference [28] describes several standardized elicitation protocols and any one of them can be incorporated to derive structured inferences for the problem. The proposed elicitation based metrics uses a combination of individual judgements, joint judgements and facilitated group discussions.

Fig. 1 shows the AWR framework overview with the corresponding resilience quadrilateral showing how implementing resilience investments results into increased anticipate, withstand and recover metrics to improve the resilience performance of the system.

The AWR metrics are the final product of the resilience analysis process and requires some preliminaries to begin. The system model is utilized in four forms; *i*) the power system model for the power flow feasibility simulations, *ii*) the threat model that defines the system degradation to defined impacts, *iii*) topological model that provides the graph

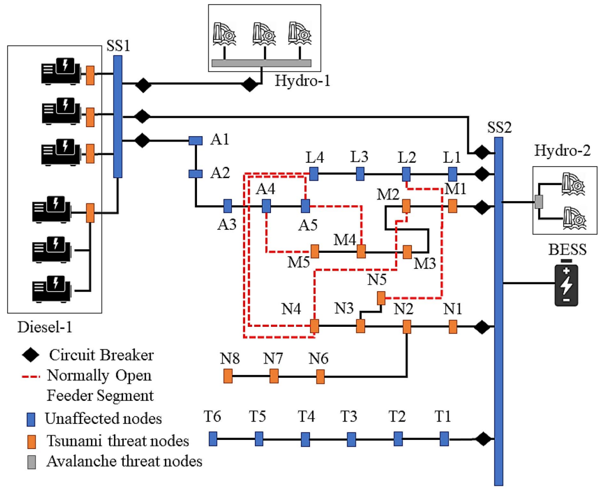

Fig. 2. Real world system showing generation resources and switches.

representation, and *iv*) the geo-spatial model to map the electrical infrastructure. Alternative planning strategies consists of a set of resilience improvement infrastructural and operational upgrades planned by the utility to be evaluated and implemented. The threat models are used to generate scenarios of the power system model with impacts realized. The system static factors is used to obtain expert and stakeholder judgements on more subjective information about the system.

A. Threat Modeling

Extreme weather events and natural disasters impact the resilience of the distribution grid and have severe long term impacts on the socio-economic condition of isolated communities like the RWS presented in this work. The RWS is susceptible to hurricanes, avalanches, tsunamis and earthquake. A previous measure to improve resilience of the RWS was an "under-grounding" effort to convert all overhead lines to underground feeders to prevent the impact of high wind speeds/hurricanes in the area. Several papers have deterministic or probabilistic tackled the problem of estimating damage in the system due to an extreme event [7]. However in this work, the system owners had a detailed inundation report due to tsunami [29] and avalanche and the proximity of each node in the system relative to the inundation region is known. An explicit modeling of failure modes of the system is performed to evaluate the conservative damage scenarios possible in the system for each threat and is shown in the system one-line in Fig. 2.

B. Improving Robustness Through Topological Factors

Robustness is defined as the ability of the network to resist damage. The robustness domain of the topological resilience can be explored effectively using graph theoretic concepts. The PDS is modeled as a graph $G = (N, E)$ with N nodes and E edges with one-to-one mapping with the system one-line. The topological robustness $\mathfrak{R}_\tau$ is computed by combination of five graph properties. The definition and the expression of the properties are given below.

1) Average Betweenness Centrality (C_B): Betweenness centrality of a node x is defined as the number of shortest paths between all pairs of nodes in the connected graph passing through the given node x. It is measure of node importance and indicates how many shortest paths are dependent on the nodes present. The average betweenness centrality provides a clue to how susceptible the graph is to perturbations or failures that can possibly sever connections between nodes as it is not favorable to have a node with high betweenness centrality fail in the system.

$$C_B(i) = \sum_{i \neq j \neq k} \frac{\sigma_{jk}(i)}{\sigma_{jk}} \tag{1}$$

where $\sigma_{jk}(i)$ refers to the number of shortest paths between leaf nodes that pass through the node i, and σ_{jk} is the total number of shortest paths in the graph.

2) Percolation Threshold (f_c): Percolation theory can be employed to study the robustness of the network. describes the infinite dimensional percolation analysis of a graph which is subject to random removal of nodes which is denotes by f. This random removal is representative of an unfavorable event. For such study, it is observed that there exists a critical fraction of nodes removed f_c for which the graph degrades into individual isolated clusters. This critical fraction of nodes is called the percolation threshold shown below as an approximation using statistical mechanics approach [30]. It is favorable for the network to have a high f_c indicating that node failures need to be larger for the system to collapse with no giant connected components.

$$f_c = 1 - \frac{1}{\kappa_0 - 1} \tag{2}$$

where, $\kappa_0 = \langle k^2 \rangle / \langle k \rangle$ and $\langle k^2 \rangle$ is the square of the standard deviation of the degree distribution of the network. The critical fraction of nodes in this graph theoretical analysis should not be confused with critical loads which are high priority loads that require non-discontinuity of service during unfavorable events. However these critical nodes are highly influential in the robustness of the system.

3) Algebraic Connectivity (λ_{alg}): Also called the Fiedler value, it is the second smallest eigenvalue of the laplacian matrix of the graph and a prime indicator of network robustness [31]. The laplacian matrix is the sum of the degree matrix D and the negative of the adjacency matrix A. The elements of the laplacian are given by

$$L_{(i,j)} = \begin{cases} deg(n_i), & \text{if } i = j \\ -1, & \text{if i} \neq \text{j and } n_i \text{ is adjacent to } n_j \\ 0, & \text{otherwise.} \end{cases} \tag{3}$$

4) Degree Distribution ($\langle k \rangle$): The degree of each node is defined as the number of adjacent nodes connected to that particular node. The degree distribution of all nodes is given by

$$\langle k \rangle = \frac{2|E|}{|N|} \tag{4}$$

the degree distribution of PDS is an indicator of topological resilience as it represents the heterogeneity of the PDS [12].

TABLE II
FACTORS IMPACTING RESILIENCE FOR ANTICIPATE METRIC

ID	Threat and vulnerability (T)			Power Delivery and Loads domain (P)			Restoration and Recovery Domain (R)		
	Weight	Factor	Data Type	Weight	Factor	Data Type	Weight	Factor	Data Type
1	0.071	Threat identification	Bool	0.091	Critical load identification	Bool	0.176	Energy storage	Bool
2	0.071	Threat analysis and documentation	Bool	0.136	Backup generators for high priority loads	Bool	0.176	Automatic restoration plan	Bool
3	0.143	Curated threat response plan	Bool	0.136	Backup generators for medium priority loads	Bool	0.118	Standby repair crew	Bool
4	0.143	Threat warning time	Int(Min)	0.182	Average runtime of backup generation	Int (Min)	0.118	Repair crew cross training	Bool
5	0.143	Threat warning accuracy	Float(%)	0.136	Fault prevention plan	Bool	0.110	Emergency staging site	Bool
6	0.214	Emergency drill	Bool	0.091	Annual vegetation management	Bool	0.102	PPE and tools	Bool
7	0.214	Maximum outage expected	Int(Min)	0.092	System asset inventory	Bool	0.100	Fuel inspection	Bool
8				0.136	Routine asset inspection	Bool	0.100	Mutual assistance program with neighboring utilities	Bool

5) Graph Diameter (D): The graph diameter is defined as the largest distance between a pair of nodes in the graph. The graph diameter is a measure of the reachability of the topology and inversely reflects the robustness, i.e., larger the diameter, smaller the robustness [32].

Once the topological resilience factors are extracted, a vector of the factors is obtained for each scenario that is analyzed. This is represented as

$$\vec{\mathfrak{R}}_\tau = \left[f_c, D, \Lambda_2, C_B, \langle k\rangle\right] \tag{5}$$

This vector represents the topological component of the resilience analysis. For each of the system configuration, threat scenarios or study cases, a new vector is created. The positive or negative impact of the vector is mapped to a impact vector D_τ given by,

$$\vec{D}_\tau = [1, -1, 1, -1, 1] \tag{6}$$

If the impact element in D_τ positive, it means larger the value of the indicator for the alternative, larger the topological robustness and if negative, vice versa. The $\mathfrak{R}_\tau$ vector is collected for all scenarios to be analyzed, i.e., basecase, damage, with and without resilience upgrades are passed through the Analytical Hierarchical Process (AHP) [33] decision making presented in Section III-D.

C. The AWR Metrics Using Resilience Factors

1) Blue Sky Operation and the Anticipate Metrics: In the normal or blue sky operating condition, it is imperative to observe the different factors that can negatively affect resilience: weather conditions, system operating states, fuel for generation, demand in systems and other intrinsic utility-specific conditions that can include crew training, emergency operating plans that effectively improves the resilience but is not captured as a network parameter. It is also important to ensure the system is sufficiently hardened against known threats in the system. A simple and flexible resilience metric is introduced at this time to evaluate the planning actions that improve the robustness of the system and enable preparedness actions through increased situational awareness and sensing.

To address the static design and operational elements that impart resilience and the real-time measurements from sensors, static factors that includes three groups of resilience capturing attributes from the main domains of physical resilience. These three domains presented in this paper are: (a) threat and vulnerability, (b) power delivery and loads, and (c) restoration and recovery. Similar approaches have been employed in extracting a unified score on interdependent complex systems such as the national health preparedness index which has served as a motivation to capture non-systemic parameters [34] and in. The static factors are very utility-dependent and require careful elicitation with the utility to identify the required domains and associated factors. In this work, the anticipate metric was devised specifically for the real world system studied and is presented in Table II. This approach allows the PDS operator and planner to assess the anticipate resilience of the system while being flexible enough to add the required resilience objective into the formulation as required. A maximum score is defined for certain factors and is evaluated as the ratio of the given response with the maximum response. The overall domain score is computed by the weighted sum of all factors as described in Section III-C. The static factor score is computed by weighted sum scoring with each domain contributing according to the rank order established through discussions with the utility.

2) Black Sky Operation and the Withstand Metrics: The second stage of the event progression is the time between the start and end of the HILF event. The "Withstand" resilience of the system is defined as the ability of the system to resist and absorb the impact of the event during the event progression while ensuring the continuity of service to the critical loads. Several operational and infrastructural techniques can be used to improve the withstand resilience of the system.

For the planning phase, infrastructural methods to enable resilience can be employed, such as adding distributed generations (DGs) to the system including storage, hardening of lines, converting overhead line to underground lines, elevation of substations. For the operational phase, dispatch of DG resources, proactive reconfiguration to reroute power to critical sources, microgrid formation, demand side management can be employed. However, in this study, we pick the resilience improvement method of adding a Battery Energy Storage System (BESS) for increasing the generation reserve in the system during the occurrence of the event.

TABLE III
FACTORS IMPACTING RESILIENCE FOR WITHSTAND METRIC

Resilience Factor	Description	Impact
Critical Load Not Lost (CLNL)	Fraction of critical loads online to total critical loads in the system	Positive
Total Available Generation (G)	Total generation available for dispatch	Positive
Critical Load Demand(D)	Operating demand of the connected critical loads	Negative
Topological Robustness($\mathfrak{R}_\tau$)	Graph theoretical robustness and absorption factors	Positive
Threat Impact Factor(TIF)	Empirical integer value that accounts for further system degradation during event progression	Negative

TABLE IV
FACTORS IMPACTING RESILIENCE FOR RECOVER METRIC

Resilience Factor	Description	Impact
Critical Load Restored (CLR)	Fraction of critical loads restored to total critical loads lost post-event	Positive
Path Redundancy (RP)	Total number of generation to critical load paths in equivalent graph representation	Positive
Generation Redundancy (RG)	Generation available	Positive
Switching Operations (SO)	Number of switching configurations required for resilient configuration	Negative
Switching Time (T_{SO})	Time to achieve resilience configuration (depends on whether switches are manual or automatic)	Negative

To quantify the withstand resilience, a vector of resilience factors was selected to analyze the system's withstand capacity. An AHP method to consolidate the withstand resilience score for each scenario. The resilience factors used are shown in Table III. The generation (G) and the critical load demand (D) are extracted from the one-line and power flow information. A power flow feasibility check in Hypersim, further elaborated in Section III-A, is performed to ensure that the power distribution system is capable of operating within the specified operational constraints. The critical load demand is obtained from the daily load profile. To capture the intensity of the weather event, a new factor called the threat impact factor (TIF) is calculated and is individually assigned for each of the threats present. The value of the threat impact factor increase with the intensity of the event. The topological robustness ($\mathfrak{R}_\tau$) computed from Section is computed for each scenario. The critical load not lost (CLNL) is the fraction of critical loads that are still operational during the event to the total number of critical loads in the system. Once the factors are assembled, an AHP is performed similarly to that of the topological robustness calculation to obtain the withstand resilience score $\mathfrak{R}_w$ for each of the scenarios as shown in Section III-D. The collection of resilience factors for each scenario is presented as a vector,

$$\vec{\mathfrak{R}_w} = [G, D, TIF, CLNL, \mathfrak{R}_\tau] \tag{7}$$

The positive or negative impact of the factors in the Withstand metrics is presented in Table III and is used to form the impact metric $\vec{D_W}$ as shown below.

$$\vec{D_W} = [1, -1, -1, 1, 1]. \tag{8}$$

3) Grey Sky and the Recover Metrics: The third stage of the event occurrence, when the threat has subsided and the system is trying to recover from the damaged state to the state of normal operation. In this stage, we introduce the "Recover" resilience metrics which quantify the ability of the system to recover from an unfavorable event. The recover metrics depends on the rapidity of restoration, redundancy of resources and resourcefulness of assets. The post-threat recovery of the system starts with the evaluation of system damage. The survey produces a damage report enumerating the number of damaged assets including poles, lines, transformers, switches, etc and the corresponding location. In this work, we consider that the system requires investments to support switching based reconfiguration.

The addition of automated switching in the distribution network adds redundancy to the network improving the recovery capacity of the system. Commercially available as distribution automation switches, these switches allow for network reconfiguration to restore service to lost loads. The planning effort in the placement of these switches improve the rapidity of restoration in the real world system studied. The resilience factors utilized for the evaluation of the recover metrics using automated switches $\vec{\mathfrak{R}_{R_{as}}}$ are shown in Table IV. The collection of resilience factors for each scenario is presented as a vector,

$$\vec{\mathfrak{R}_R} = [RG, RP, CLR, SO, T_{SO}] \tag{9}$$

The positive or negative impact of the factors in the Recover metrics is presented in Table IV and is used to form the impact metric $\vec{D_R}$ as shown below.

$$\vec{D_R} = [1, 1, 1, -1, 1] \tag{10}$$

Similar to the withstand metric, AHP is used to compute composite recover resilience metric $\mathfrak{R}_R$ for each of the scenarios as shown in Section III-D.

III. USING RESILIENCE METRICS TO SUPPORT PLANNING AND OPERATIONAL DECISIONS

This section will explain the computation methodology for the AWR metrics and its use by planners to plan for resilience boosting investments and increase operational resilience.

A. Real-World Distribution System for Validation

The AWR metric was developed for a remote distribution system network in Cordova, Alaska referred heretofore as the Real World System (RWS) however can be modified to any utility irrespective of configuration, customer profile, geography and capabilities. The RWS is an isolated PDS with no connection to the bulk grid and is served by two substations SS1 and SS2 with one Diesel, two Hydro-electric plants both of with are utility-owned. The one-line of the RWS is shown below in Fig. 2. Each node in the system is a double ended switch with loads connected downstream, i.e., the nodes can disconnect on either ends to be served by either SS1 or

SS2 to accept service through the normally open lines (shown in dashed red lines). The physical model is simulated using Hypersim, with the a supplemental graph theoretical model built in MATLAB. The MATLAB and Hypersim models interact through a Python event generator for the generation of data, extraction of resilience factors, formation of topology and calculation of resilience metrics as shown below. More details and a similar application based on the setup is presented in our previous work [35].

The explicit threat models and the electrical response to said models were studied using the Scopeview in HYPERSIM [36]. HYPERSIM and Scopeview are tools from OPALRT system. Events have different topological (electrical), effect on the power system depending upon, type, location, magnitude of the event. Communication link to control the HYPERSIM simulation was created using API in Python. With the Python API, a user input triggers the model to run in base case mode and in the degraded scenarios. The Python API simultaneously conveys the event information to resiliency computation engine, computes the resiliency scores for the system experiencing particular events.

B. Defining and Selecting Resilience Planning Investments Through AWR Metrics

The distribution utility can adopt a number of planning measures to enable resilience in the system. These upgrades can take the form of infrastructure hardening, situational awareness, redundancy and resource allocation. Infrastructure hardening by far the most adopted method by utilities to securing the infrastructure against damage due to threats. This includes increasing the strength of poles against wind damage, "undergrounding" of conductors, and elevating substation to mitigate flooding [37]. Situational awareness increases the window of action for operators to implement mitigation strategies. This includes better threat sensing mechanism like earthquake early warning systems, tsunami buoys, and hurricane damage characterization and prediction. Redundancy is the form of more alternative electric path availability through the addition of backup feeder lines or switching. Source redundancy and availability improves the chance of the system surviving HILF events [38].

The planner can use any of the strategies used in Table V to use. The control actions selected and studied in this paper may not apply to all utilities due to multiple factors including budget constraints, age of existing infrastructure, engineering difficulties, experience differences in utility staff and need to be determined specific to a given system. In this work, we assume that the utility has an option of implementing a combination of these resilience improving investments that are combined together as Resilience Planning Investments (RPI). Each RPI provides a targeted approach to improve situational awareness and preparedness, robustness, resourcefulness and rapidity and are assumed to be determined through careful considerations of investment heuristics as shown in Fig. 3 along with the evaluation phase. The investment must satisfy the level and scope of resilience defined along with the budgetary constraints. The formulation of these RPIs are beyond the scope of this paper. RPIs, aside from the nature of the risk, type of PDS, budgets, solutions and regulations, can even vary based on the organization of the utility. An RPI for a investor-owned utility maybe different from that of one for an electric cooperative, public utility or a federal utility [39].

Once the RPI options are available, the three metrics can be employed to determine the best option through the evaluation phase. The RPIs developed for the system have the three components, RPI_A, RPI_W, and RPI_R, that are measured by the AWR metrics. This ensures that aspects of the system's resilience profile are not overlooked due to the focus on a particular dimension of resilience. The Anticipate component RPI_A increases situational awareness and preparedness. The Withstand component RPI_W ensures the survival of critical loads during the event and the recover component RPI_R ensures the recovery of the system to pre-event levels after the event has subsided. The calculation methodology is shown in Section III-C and III-D.

TABLE V
RESILIENCE ENABLING INVESTMENTS FOR DISTRIBUTION SYSTEMS

Upgrade approach	Specific measures
System hardening	Converting overhead line to underground Elevating substations Relocating feeders closer to roads for easier repairs Adding redundant feeders Infrastructure replacement Increasing strength of above grade equipment
Resource management	Increase available generation (more distributed generation and storage) Demand response Microgrids
Reconfiguration	Additional switches Network reconfiguration Mobile power sources
Situational awareness	Advanced Metering infrastructure Micro-PMU Advanced weather prediction

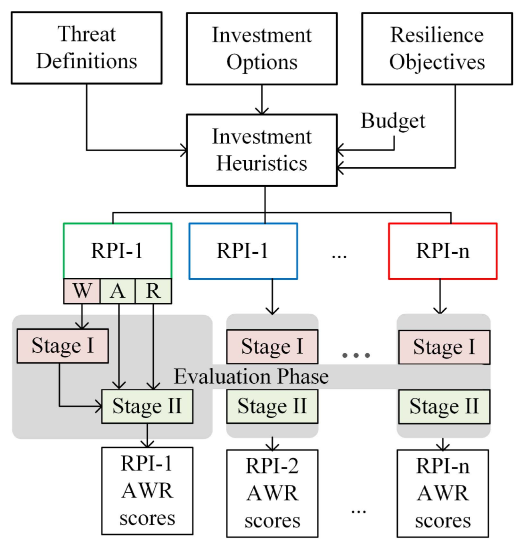

Fig. 3. Overview of selecting Resilience Planning Investments.

TABLE VI
RESILIENCE PLANNING INVESTMENT OPTIONS

Investment	RPI-1	RPI-2	RPI-3	RPI-4
Early Warning system (Tsunami Avalanche)	x	x	x	x
Backup generation for priority loads	x		x	x
Automatic restoration plan			x	x
Back-side tie	x	x		x
Automated switching	x		x	
BESS Option 1	x			x
BESS Option 2		x		

Once the threat and vulnerability assessment is performed, the different probable scenarios that can impact the systems are cataloged. The RPI$_W$ used in this first stage is the addition of the Battery Energy Storage System (BESS). The idea location of the BESS in the RWS is based on the most central node SS2 as shown in Fig. 2. The stage I plan provides the most resilient configuration of the system with the BESS at SS2. This resultant system provides the baseline improvement in withstand resilience. This allows for the system to be further evaluated for resilience improvements using RPIs in the second stage to increase preparedness using the $\Re_A$ and the rapidity of restoration using the $\Re_R$ metric.

The output of stage I provides the best resilience investment that improves withstand metric. The new baseline system where the RPI$_W$ is implemented on is used to evaluate the RPI$_A$ and RPI$_R$.

C. Computation of Anticipate Metric for RWS

As presented in Table I, the different static factors based on utility elicitation are used to compute the resilience of preparedness and anticipation. For the test system, the approach of utilizing anticipate metric is based on the threats that the system experiences. For the RWS, the threats that are being analyzed are tsunami, earthquake, avalanche, and volcano with each affecting different parts of the system. The direct modeling of system threats allows for simplifying the planning process. For each threat, the domain scores and computed and a weighted sum score is calculated using the equation,

$$\Re_A = \sum_{i=1}^{N} T_i W_i^T + \sum_{i=1}^{N} P_i W_i^P + \sum_{i=1}^{N} R_i W_i^R \tag{11}$$

where $\Re_A$ is the anticipate metric score, T_i and W_i^T are the score and weight of the threat and vulnerability domain, P_i and W_i^P are the score and weight of the power delivery and loads domain, and R_i and W_i^R are the score and weight of the recovery and restoration domain.

However, the main requirement for increased anticipate resilience is the presence of advanced telemetry and sensing for the warning of impending threat to the system. We assume that early-warning threat detection is installed in place for the system and that warning triggers a calculation of anticipate metric score. The assumption also includes a robust and reliable communication system that will allow for successful transmission of the warning to the operations center. The system operator can decide the move the system from normal operating mode to the alert mode and can prescribe proactive control actions to mitigate the impact of the event. The planning operation can also be studied through the anticipate metric by measuring the impact of adding a new preparedness and anticipation resource to the system and comparing the anticipate score to the base case calculated.

D. Computation of Withstand and Recover Metric for RWS

The withstand metric and recover metrics are assessed through analytical hierarchical process for each scenario with and without the resilience investment implemented for varying degrees of degradation. For the AHP analysis,the weights are not explicitly defined but are selected through developing a pairwise comparison matrix (PCM) which is the matrix of the impact of the each of the factors on the system resilience. It is a 'n x n' matrix where 'n' is the number of factors being studied. Say element 1 in the vector $\vec{\Re}_W$ is the number of critical loads lost and element 3 is the available collected generation. The system is more resilient when the number of critical loads lost is low than when the available connected generation is low. therefore the element (1, 3) would be greater than 1 and the element (3, 1) would be the inverse of element (1, 3).

$$M_{pc} = \begin{bmatrix} c_{1,1} & \cdots & c_{n,1} \\ \vdots & \ddots & \vdots \\ c_{1,m} & \cdots & c_{n,m} \end{bmatrix} \tag{12}$$

$$c_{i,j} = c_{j,i}^{-1} \text{ for } i \neq j \tag{13}$$

$$c_{i,i} = 1 \tag{14}$$

Linear transformation of the elements based on the positive or negative performance of the factor on the resilience of the system. The weights of the factors similar to equation (1) are calculated from the normalized principal eigenvector of the PCM. The weights represent the impact of the factors on the resilience of the system. The sum of product of the weights with the linear transformation element gives the composite score. AHP is used in the computation of topological resilience, recover metrics and withstand metrics. The linear transformation is given by:

$$\rho_{i,j} = \frac{c_{i,j} - \min_{i=1}^{n}(c_{i,j})}{\max_{i=1}^{n}(c_{i,j}) - \min_{i=1}^{n}(c_{i,j})} \tag{15}$$

for improvement in resilience for a higher value of $c_{i,j}$, where i is the alternative and j is the criteria.

$$\rho_{i,j} = \frac{\max_{i=1}^{n}(c_{i,j}) - c_{i,j}}{\max_{i=1}^{n}(c_{i,j}) - \min_{i=1}^{n}(c_{i,j})} \tag{16}$$

for reduction in resilience for a higher value of $c_{i,j}$. With the weights and the linearized performance scores obtained, the resilience score is calculated by,

$$\Re_{\mathrm{i}} = \sum_{j=1}^{N} \rho_{i,j} W_i \tag{17}$$

Similarly, for the recover metric, the scenarios present the alternatives from each of which the vector $\vec{\Re}_R$ is extracted. The AHP presents the composite score on the system recovery resilience.

TABLE VII
WITHSTAND METRICS RESULTS FOR RWS UNDER TSUNAMI THREAT

Case No	Description of event	Resilience Score ($\mathfrak{R}_\mathbf{w}$)		Comments on Resiliency score
		Without Battery	With Battery (100% SOC)	
1	Fault on Feeder M	0.70929	0.7528	• Loss of large number of critical loads on Feeder M • Change in topology affected topological robustness factors
2	Loss of single CL on Feeder M	0.9382	0.97364	• Loss of single CL • No network change • Scenario models the load as being disconnected
3	Fault on Feeder N	0.86067	0.90596	• Loss of large number of CL on Feeder N • Score is higher than Case 1 because of the number, size of load and priorities of CLs lost
4	Loss of single CL on Feeder N	0.89958	0.94704	• Loss of single CL Lower score than Case 2 because of the size of the CL
5	Loss of Diesel Gen	0.66902	0.72494	• Loss of diesel generation
6	Loss of Diesel Plant, Hydro-1 in SS1 and fault on Feeder M	0.35612	0.3678	• Loss of large Hydro and Diesel generation along with loss of CLs on Feeder M Worst case scenario • Contributions from BESS system does not increase resilience score due to loss of large generation capacity.

E. Evaluating Operational Resilience for Decision Support

Selecting most appropriate operational decisions are required to maximize AWR resilience. The operational decision can encompass both proactive and reactive decisions. Some of these have been explored by the authors in the past. In [40], a resiliency driven approach to proactive reconfigure the system by eliminating vulnerable feeders and transferring their loads to more robust feeders was presented. In [35], a resilience based BESS dispatch was presented and a clear improvement in overall resiliency and service to critical loads by proactively charging BESS forgoing economic operation. Similar to evaluating RPIs, Withstand and Recover metrics can evaluate proactive and corrective control actions similar to [35], [40].

IV. RESULTS AND DISCUSSIONS

A. Resilience Investment Plans for the RWS

The resilience of the Cordova grid in Alaska to the tsunami, avalanche, earthquake and hurricane threats are evaluated. Resilience investment plans are created for the two stage approach. The RPI_W is the use of the battery to alleviate generation stress during HILF events. The anticipate metric is evaluated for RPI_A that include (a) the inclusion of a tsunami early warning and avalanche alert system (subfactors for each of the threat in T4), (b) provisions for backup generation for priority loads (P2, P3), and (c) automatic restoration plan (R2) from Table II. RPI_R is the addition of automated switches at locations T6-N4 and T3-N5 shown in Fig. 2.

B. Stage I Planning Results—Improving Withstand Resilience Using BESS

Addition of a BESS to SS-2 was the primary RPI_W analyzed for the RWS. A detailed analysis of low and high impact threats and the corresponding withstand metric scores for each scenario are shown in Table VII. The simulation was performed for cases with and without the BESS. The results from the AHP analysis indicates that the increase in withstand resilience of the system due to the presence of the battery. Comparatively, the results also indicate the change in scores is based on how the various scenarios are compared against one another. The scenarios 1 and 3 are very similar events (loss of a single critical load) that in this analysis, show that the scenario 3 fairs well for the system because of the number and size of the critical loads is higher in scenario 1 than in 3. Similarly, scenarios 2 and 4 validate the same with different scores that reflect the size and priority of the critical loads that are lost. Thus, a DNO would be able to create different scenarios based on the resilience use case of the system and would be able to make the best choice for planning and develop a business case for that resilience improvement. In scenario 6, where there is the worst case impact due to loss of generation and critical load, the 1 MW battery system has very little impact on the system resilience since the system is already highly degraded. For such a case, the DNO should look at other resilience enabling methods, especially system hardening to prevent the occurrence of the worst case scenario.

C. Stage II Planning Results

1) Improving Anticipate Metrics: For the RWS, the static factors form the base of the anticipate metric are derived through thorough elicitation between the planners, operators and engineers. We expect the anticipate metric to be the most subjective of the introduced metrics as they are system-specific, but are flexible to accommodate future factors to assess system preparedness and anticipation for threats affecting the system. The RWS utility can study the improvement in resilience metrics by utilizing anticipate metric worksheet with each factor represented by their domain and corresponding ID. The anticipate metric calculations for the addition of the static factors P2, P3, T4, R2 and the results are shown in Table VIII.

2) Improving Recover Metrics: The RII used to demonstrate the flexibility of the AWR metric to accommodate any resilience enabling strategy and to provide decision support, is the planning study for the addition of automation of switches.

TABLE VIII
RESULTS OF ANTICIPATE METRIC ANALYSIS COMPARING DIFFERENT UPGRADES

	Base Case	T4	P2,P3	R2	All
T	0.588	0.8115	0.588	0.588	0.8115
P	0.547	0.547	0.7239	0.547	0.7239
R	0.8045	0.8045	0.8045	0.8868	0.8868
RA	0.5675	0.67925	0.65595	0.5675	0.7677

TABLE IX
RECOVER METRICS SCORES

Case 1A	Case 1B	Case 2A	Case 2B
6.1558	6.5412	5.2828	6.1174

In the RWS, additional automated switches were places in T6-N4 and T3-N5. The installation of these additional switches will introduce additional feasible networks creating more paths to supply the cumulative critical load in the network. It is assumed that a fault has occurred in section SS2-N1 and results in the outage of all N feeder nodes. Two planning scenarios with additional automated switches are proposed and the appropriate feasible networks are calculated for each of them. It should be noted that some resilient topologies are infeasible due to power flow constraints. The cases were created based on the additional switches and the resiliency factors of each case was extracted and passed on to the AHP computation to calculate the $\mathfrak{R}_R$ scores. For the recover metrics analysis, we created 2 threat cases with and without automated switching schemes for restoration. The first threat case (Case 1A/B) is similar to the one explained for the withstand case where a tsunami causes inundations of loads and switches along the coast and the second threat case (Case 2A/B) is an avalanche case where the system loses hydro generation due to the snow blocking the run of the river. The results of the recover metric analysis is shown in Table IX.

The DNO is then able to select a restoration path that allows for the downed loads to be picked up. We compare the different recover resilience factors for the selected restorations scheme to analyze the increase in recover resilience score to the installation of automated switches in the most critical restoration paths.

D. Selection of Most Resilient Planning Investment

Once stage I and stage II evaluations are complete, the resultant highest composite AWR score is chosen as the most resilience RPI. The plot of the RPI resilience scores shown in Fig. 4 shows AWR metrics for the different phases of the event progression. The results indicate that RPI-1 is the best alternative among the candidates for its high overall AWR score. The increase is predominantly due to high anticipate score and recover score even though it shows lower withstand resilience than RPI-2. However, RPI-2 shows higher anticipate score also, showing a higher operational resilience due to improved preparedness measured by $\mathfrak{R}_A$.

Therefore in the two stage approach, the planner can now select between RPI-1 and RPI-2 based on budgetary constraints in each plan. Budget has not been added for this work but it may be more realistic to include a cost function to eliminate the selection of a economically infeasible resilience upgrade. Also, some of the upgrades can be prohibitively expensive and show only marginal improvements in the AWR.

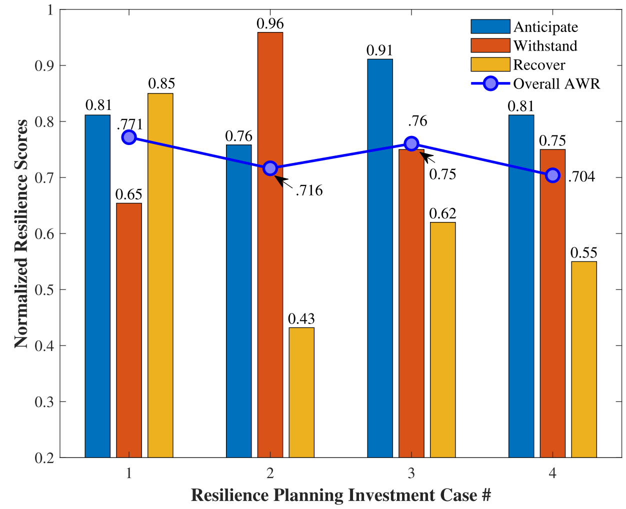

Fig. 4. AWR results for different investment plans.

E. Operational Decision Support

Operational resilience can be achieved by selecting decisions that increase the AWR scores. Selection of best switching sequence for the re-energization of the outage area, de-emphasizing economic operation over resilient operation in the dispatch of DER sources, proactive reconfiguration to remove vulnerable feeders from the extreme event path, alleviating generation stress through AMI based load curtailment for supporting critical loads can be studied through the AWR metrics similar to some of the results reported in Table VII.

V. CONCLUSION

This work presents novel Anticipate-Withstand-Recover (AWR) resilience metric algorithms considering event progression to allow electric utilities to evaluate system resilience performance before, during and after the extreme event. The AWR metrics computes a composite resilience score for each stage of event progression that is easy to understand, flexible and comprehensive. Developed AWR metrics supports the planning and operation of resilient distribution networks. The anticipate metric uses system elicitation to capture all the resilience factors that are not typically captured by sensor networks and real-time measures including weather, threat warning, preparedness, resources, and emergency action plans. The withstand metrics computes the systems ability to absorb and maintain performance during extreme event and allows for the Distribution Network Operator (DNO) to assess planning measures to improve resilience. The recover metric computes the resilience parameters that captures the recovery and rapidity of restoration of the system. The use of Analytical Hierarchical Process (AHP) and Weighted Sum

Model (WSM) for the computation of AWR scores is intuitive and flexible for DNO and planners to approach the metric formulation in a subjective manner in accordance to the characteristics of the distribution network. The AWR metric was validated for a real world power distribution system modeled in a real-time and was demonstrated to show the improvement in situational awareness with anticipate metric, improvement in ability to serve critical loads with minimal interruptions using withstand metric and improvement in rapidity and maximum restoration using the recover metric. Future work will include extending the operational resilience through optimization based decision support that maximize the AWR metrics over the set of available control actions pre- and post-event.

ACKNOWLEDGMENT

Support from CEC, Alaska is much appreciated for providing data for validation. Thanks to S. Chanda, L. Jia, R. Hovsapian and I. Diahovchenko, who helped to shape this work.

REFERENCES

[1] F. Robles, *Puerto Rico Spent 11 Months Turning the Power Back On. They Finally Got to Her*, New York Times, New York, NY, USA, Aug. 2018. [Online]. Available: https://www.nytimes.com/2018/08/14/us/puerto-rico-electricity-power.html

[2] A. Kwasinski, F. Andrade, M. J. Castro-Sitiriche, and E. O'Neill-Carrillo, "Hurricane maria effects on Puerto Rico electric power infrastructure," *IEEE Power Energy Technol. Syst. J.*, vol. 6, no. 1, pp. 85–94, Mar. 2019.

[3] K. E. Swartz. *Texas Blackouts Highlight Threats to Southeast Grid*. Accessed: Mar. 2021. [Online]. Available: https://www.eenews.net/energywire/stories/1063727073

[4] P. Dehghanian, S. Aslan, and P. Dehghanian, "Quantifying power system resiliency improvement using network reconfiguration," in *Proc. IEEE 60th Int. Midwest Symp. Circuits Syst. (MWSCAS)*, 2017, pp. 1364–1367.

[5] S. Mousavizadeh, M.-R. Haghifam, and M.-H. Shariatkhah, "A linear two-stage method for resiliency analysis in distribution systems considering renewable energy and demand response resources," *Appl. Energy*, vol. 211, pp. 443–460, Feb. 2018.

[6] H. Zhang, Z. Bie, G. Li, and Y. Lin, "Assessment method and metrics of power system resilience after disasters," *J. Eng.*, vol. 2019, no. 16, pp. 880–883, 2019.

[7] M. Panteli, P. Mancarella, D. N. Trakas, E. Kyriakides, and N. D. Hatziargyriou, "Metrics and quantification of operational and infrastructure resilience in power systems," *IEEE Trans. Power Syst.*, vol. 32, no. 6, pp. 4732–4742, Nov. 2017.

[8] D. Shelar, S. Amin, and I. Hiskens, "Evaluating resilience of electricity distribution networks via a modification of generalized benders decomposition method," *IEEE Trans. Control Netw. Syst.*, vol. 8, no. 3, pp. 1225–1238, Sep. 2021.

[9] B. M. Ayyub, "Practical resilience metrics for planning, design, and decision making," *ASCE/ASME J. Risk Uncertainty Eng. Syst. A Civil Eng.*, vol. 1, no. 3, 2015, Art. no. 04015008.

[10] S. Chanda, A. K. Srivastava, M. U. Mohanpurkar, and R. Hovsapian, "Quantifying power distribution system resiliency using code-based metric," *IEEE Trans. Ind. Appl.*, vol. 54, no. 4, pp. 3676–3686, Jul./Aug. 2018.

[11] P. Bajpai, S. Chanda, and A. K. Srivastava, "A novel metric to quantify and enable resilient distribution system using graph theory and choquet integral," *IEEE Trans. Smart Grid*, vol. 9, no. 4, pp. 2918–2929, Jul. 2018.

[12] S. Chanda and A. K. Srivastava, "Defining and enabling resiliency of electric distribution systems with multiple microgrids," *IEEE Trans. Smart Grid*, vol. 7, no. 6, pp. 2859–2868, Nov. 2016.

[13] A. Gholami, T. Shekari, M. H. Amirioun, F. Aminifar, M. H. Amini, and A. Sargolzaei, "Toward a consensus on the definition and taxonomy of power system resilience," *IEEE Access*, vol. 6, pp. 32035–32053, 2018.

[14] A. R. Berkeley and M. Wallace, *A Framework for Establishing Critical Infrastructure Resilience Goals*, Nat. Infrastruct. Adv. Council, New York, NY, USA, 2010.

[15] E. Vugrin, A. Castillo, and C. Silva-Monroy, "Resilience metrics for the electric power system: A performance-based approach," Sandia Nat. Lab., Albuquerque, NM, USA, Rep. SAND2017-1493, 2017.

[16] G. Kandaperumal and A. Srivastava, "Resilience of the electric distribution systems: Concepts, classification, assessment, challenges, and research needs," *IET Smart Grid*, vol. 3, no. 2, pp. 133–143, 2019.

[17] Y. Wang, C. Chen, J. Wang, and R. Baldick, "Research on resilience of power systems under natural disasters—A review," *IEEE Trans. Power Syst.*, vol. 31, no. 2, pp. 1604–1613, Mar. 2016.

[18] G. P. Cimellaro, A. M. Reinhorn, and M. Bruneau, "Framework for analytical quantification of disaster resilience," *Eng. Struct.*, vol. 32, no. 11, pp. 3639–3649, 2010.

[19] J. Lu, J. Guo, Z. Jian, Y. Yang, and W. Tang, "Resilience assessment and its enhancement in tackling adverse impact of ice disasters for power transmission systems," *Energies*, vol. 11, no. 9, p. 2272, 2018.

[20] G. Fu *et al.*, "Integrated approach to assess the resilience of future electricity infrastructure networks to climate hazards," *IEEE Syst. J.*, vol. 12, no. 4, pp. 3169–3180, Dec. 2018.

[21] P. Stockton, *Resilience for Black Sky Days: Supplementing Reliability Metrics for Extraordinary and Hazardous Events*, Nat. Assoc. Regul. Utility Commissioners, New York, NY, USA, 2014.

[22] J. Monken, "Black sky: Exposing electricity as the achilles' heel of resilience," *J. Bus. Continuity Emerg. Plan.*, vol. 9, no. 1, pp. 25–30, 2015.

[23] M. Panteli and P. Mancarella, "Modeling and evaluating the resilience of critical electrical power infrastructure to extreme weather events," *IEEE Syst. J.*, vol. 11, no. 3, pp. 1733–1742, Sep. 2017.

[24] D. N. Trakas, M. Panteli, N. D. Hatziargyriou, and P. Mancarella, "Spatial risk analysis of power systems resilience during extreme events," *Risk Anal.*, vol. 39, no. 1, pp. 195–211, 2019.

[25] X. Chen, S. Member, J. Qiu, L. Reedman, and Z. Y. Dong, "A statistical risk assessment framework for distribution network resilience," *IEEE Trans. Power Syst.*, vol. 34, no. 6, pp. 4773–4783, Nov. 2019.

[26] R. Nateghi, "Multi-dimensional infrastructure resilience modeling: An application to hurricane-prone electric power distribution systems," *IEEE Access*, vol. 6, pp. 13478–13489, 2018.

[27] M. Dumas, B. Kc, and C. I. Cunliff, "Extreme weather and climate vulnerabilities of the electric grid: A summary of environmental sensitivity quantification methods," Oak Ridge Nat. Lab., Oak Ridge, TN, USA, Rep. ORNL/TM-2019/1252, 2019.

[28] A. O'Hagan, "Expert knowledge elicitation: Subjective but scientific," *Amer. Stat.*, vol. 73, no. s1, pp. 69–81, 2019.

[29] D. Nicolsky, E. Suleimani, and R. Koehler, "Tsunami inundation maps of Cordova and Tatitlek, Alaska," *Alaska Division Geol. Geophys. Surveys Rep. Invest.*, vol. 1, p. 49, Jul. 2014.

[30] F. Radicchi, "Predicting percolation thresholds in networks," *Phys. Rev. E, Stat. Phys. Plasmas Fluids Relat. Interdiscip. Top.*, vol. 91, no. 1, Jan. 2015, Art. no. 010801. doi: 10.1103/PhysRevE.91.010801.

[31] A. Jamakovic and P. Van Mieghem, "On the robustness of complex networks by using the algebraic connectivity," in *Proc. Int. Conf. Res. Netw.*, 2008, pp. 183–194.

[32] A. Vázquez and Y. Moreno, "Resilience to damage of graphs with degree correlations," *Phys. Rev. E, Stat. Phys. Plasmas Fluids Relat. Interdiscip. Top.*, vol. 67, no. 1, 2003, Art. no. 015101.

[33] T. L. Saaty, "Decision making—The analytic hierarchy and network processes (AHP/ANP)," *J. Syst. Sci. Syst. Eng.*, vol. 13, no. 1, pp. 1–35, 2004.

[34] M. Stoto, "Measuring and assessing public health emergency preparedness," *J. Public Health Manag. Practice*, vol. 19, no. S2, pp. S16–S21, 2013.

[35] S. Pandey, S. Srivastava, G. Kandaperumal, A. K. Srivastava, M. U. Mohanpurkar, and R. Hovsapian, "Optimal operation for resilient and economic modes in an islanded alaskan grid," in *Proc. IEEE Power Energy Soc. Gen. Meeting (PESGM)*, 2020, pp. 1–5.

[36] Hypersim. *Real-Time Simulator*. [Online]. Available: https://www.opal-rt.com/systems-hypersim/ (Accessed: Aug. 20, 2021).

[37] S. Ma, L. Su, Z. Wang, F. Qiu, and G. Guo, "Resilience enhancement of distribution grids against extreme weather events," *IEEE Trans. Power Syst.*, vol. 33, no. 5, pp. 4842–4853, Sep. 2018.

[38] I. Diahovchenko, G. Kandaperumal, and A. Srivastava, “Distribution power system resiliency improvement using distributed generation and automated switching,” in *Proc. IEEE 6th Int. Conf. Energy Smart Syst. (ESS)*, 2019, pp. 126–131.

[39] L. Schwartz, *Utility Investments in Resilience of Electricity Systems*, Lawrence Berkeley Nat. Lab., Berkeley, CA, USA, 2019.

[40] S. Pandey, S. Chanda, A. Srivastava, and R. Hovsapian, “Resiliency-driven proactive distribution system reconfiguration with synchrophasor data,” *IEEE Trans. Power Syst.*, vol. 35, no. 4, pp. 2748–2758, Jul. 2020.

Gowtham Kandaperumal (Member, IEEE) received the master’s degree in electrical engineering from Arizona State University in 2014, and the Ph.D. degree in electrical engineering and computer science from Washington State University in 2021. He is a Senior Engineer with the Reliability Group, Commonwealth Edison (ComEd). Prior to ComEd, he was a Distinguished Graduate Research Fellow with Pacific Northwest National Laboratory from 2019 to 2021. He was an Electrical Engineer with Affiliated Engineers, Inc., from 2014 to 2017.

Shikhar Pandey (Member, IEEE) received the bachelor’s degree in electrical engineering from the National Institute of Technology, Patna, in 2013, and the M.S. and Ph.D. degrees in electrical engineering from Washington State University, Pullman, in 2017 and 2020, respectively. He is a Senior Engineer with the Emerging Technologies Group, Commonwealth Edison. From 2013 to 2015, he worked as a Senior Electrical Engineer with Larsen and Toubro ECC, Kullu, India. His research interests includes microgrids, smart grids, planning and operations, and synchrophasor technology and its applications.

Anurag Srivastava (Senior Member, IEEE) received the Ph.D. degree in electrical engineering from the Illinois Institute of Technology in 2005. He is the Raymond J. Lane Professor and the Chairperson of the Computer Science and Electrical Engineering Department, West Virginia University. He was an Associate Professor with the School of Electrical Engineering and Computer Science, Washington State University, Pullman, WA, USA. He has coauthored more than 300 technical publications. His research interests include data-driven algorithm for the power system operation and control. He is a IEEE Distinguished Lecturer. He is an Editor of the IEEE Transactions on Smart Grid and IEEE Transactions on Power Systems.